Generalized OFDM

Myungsup Kim and Do Young Kwak
Dept. of Mathematical Sciences, KAIST,
Deajeon, Korea
{myungsup, kdy}@kaist.ac.kr

Abstract— In this paper, a generalized OFDM (G-OFDM) which protects the out of band (OOB) leakage and satisfies the orthogonality between subcarriers is proposed for next generation wireless communications. This scheme maps many data symbols to many subchannels through filter matrix, unlike the conventional OFDM that maps a data symbol to a subchannel in a one-to-one fashion. In G-OFDM, the filter matrix is used in order to limit the OOB leakage of the spectrums of input data, which is generated through processes such as jump-removing, filtering, and orthogonalizing a specially chosen initial matrix. G-OFDM is compared with OFDM in view of OOB leakage, crest factor, complementary cumulative distribution function, and bit error rate (BER) performance.

Index Terms—Matrix filter; pilot vector; jump-removing matrix; G-OFDM; frequency; multiplexing; OFDM; BER; crest factor; CCDF.

I. Introduction

OFDM plays a significant role in modern telecommunications due to its wide ranging applications from its use in home communication technologies to wireless local area network (WLAN) [1] and mobile communication systems. This is because OFDM uses spectral resources effectively through overlapping the subcarriers while maintaining orthogonality, and it can estimate the communication channel easily using pilot symbols [2]. Furthermore, OFDM can be used to increase the channel capacity significantly using multiple input multiple output (MIMO) technology through which several users can communicate simultaneously through multiple channels on the same bandwidth using space diversity [3]. Nowadays, OFDM has been utilized in almost all areas such as mobiles, local area networks, broadcasting, and satellite communications; it will continue to be a major technology in the future. However, the spectral environment for communication will become increasingly worse because numerous systems will be connected to internet through fixed and mobile wireless communication networks. Therefore, it will be a significant problem to solve the interference between communication systems. Recently, many efforts have been focused on studies of new transmission schemes to enhance the spectral characteristics of OFDM for next generation mobile communications [4-7]. Filter bank multi-carrier (FBMC), universal filtered multi-carrier (UFMC), and generalized frequency division multiplexing (GFDM) are prominent outcomes in reducing the spectral leakage of OFDM. FBMC has the merit of being able to satisfactorily reduce the spectral leakage to neighbor channels through filtering in the frequency domain, but it uses samples two or four times per symbol, which may be a drawback in high-speed transmission because the frame lengths increase in doing so. UFMC is a scheme that mitigates the spectral leakage through filtering using Dolph-Chebyshev filters. However, many IFFT processors and filters are required for a symbol transmission, and the use of the FFT processor with twice the length of the IFFT used in the transmitter in a receiver is a factor that increases the complexity of implementation. In addition, since the response of the filter of the transmitter becomes long, the interval between the symbols may be very close to each other, so there may be a possibility of overlapping between symbols in a multipath environment. GFDM is also an effective scheme to reduce the spectral leakage. However, since the frequency bands of subcarrier are designed to overlap, it causes self-interference, which may increase the complexity of the receiver because it must implement the means to remove it [8]. In this paper, we introduce G-OFDM that can effectively reduce the spectral spread that occurs in OFDM without changing the structure of OFDM. Because G-OFDM performs filtering through filter matrices in the frequency domain with minimal operational complexity and it does not increase the length of the OFDM symbol, it is not only a spectral and power efficient modulation scheme, but also it can be operated at high speed and is compatible with the existing systems using OFDM.

In section II, we introduce the concept of G-OFDM and the generation of filter matrix that constitutes G-OFDM. Unlike OFDM that one subcarrier is created using one frequency, one subcarrier in G-OFDM is created by synthesizing several frequencies. By performing the filtering operation in the frequency domain, G-OFDM does not increase the length of the OFDM symbol in the time domain. In section III, we introduce a method for inserting pilot vectors into the filter matrix to estimate the communication channel. In section IV, we analyze the characteristic of G-OFDM that can reduce the OOB leakage. In section V, we evaluate the upper bound of the crest factor and complementary CDF for G-OFDM. In section VI, we obtain the BER performance of G-OFDM over AWGN (Additive White Gaussian Noise) channel. In section VII, we summarize the features of G-OFDM described in all previous sections.

II. G-OFDM

In G-OFDM as shown in Fig. 1, a data vector $\mathbf{d}$ is divided into J shorter vectors $\mathbf{d}_0, \mathbf{d}_1, \ldots, \mathbf{d}_{J-1}$, each of which is multiplied by the filter matrix $\mathbf{G}$, which are denoted as $\mathbf{v}_0, \mathbf{v}_1, \ldots, \mathbf{v}_{J-1}$. The k-th data symbol in the l-th data vector is carried on the k-th column of the filter matrix $\mathbf{G}$. The condition for orthogonality to recover the data symbols without interference between symbols is $\mathbf{G}^H\mathbf{G} = \mathbf{I}$. In G-OFDM as shown in Fig. 1, a data vector $\mathbf{d}$ is divided into J shorter vectors $\mathbf{d}_0, \mathbf{d}_1, \ldots, \mathbf{d}_{J-1}$, each of which is multiplied by the filter matrix $\mathbf{G}$, which are denoted as $\mathbf{v}_0, \mathbf{v}_1, \ldots, \mathbf{v}_{J-1}$. The k-th data symbol in the l-th data vector is carried on the k-th column of the filter matrix $\mathbf{G}$.

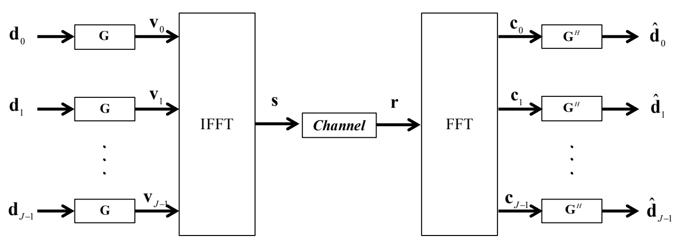

Fig. 1. G-OFDM

It is not simple to make a filter matrix $\mathbf{G}$ with good spectral and orthogonal characteristics at once, so we generate the filter matrix from an initial matrix $\mathbf{G}^{(0)}$ through the procedure depicted in the signal flow diagrams in Figs. 2. We can obtain a filter matrix

$$\mathbf{G} = f\left(\mathbf{W}^T\mathbf{F}\,\mathbf{\Psi}\mathbf{\Phi}\,\mathbf{F}^{-1}\mathbf{W}\mathbf{G}^{(0)}\right), \tag{1}$$

where

$$f(\mathbf{K}) = \mathbf{K}\left(\mathbf{K}^H\mathbf{K}\right)^{-\frac{1}{2}}. \tag{2}$$

The two matrices $\mathbf{\Phi}$ and $\mathbf{\Psi}$ remove the jump components and filter all the columns of the incoming data matrix, respectively so that their spectrums are forced to be zeros at the beginning and end of the frequency band.

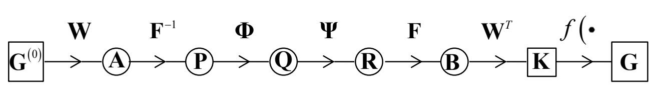

Fig. 2. Signal flow diagram for filter matrix generation

A. Initial Matrix

An initial matrix is constructed so that all the columns have two minimum nonzero entries, are unit vectors, and are orthogonal to each other. For an odd N, we define an initial matrix

$$\mathbf{G}^{(0)} \equiv \begin{bmatrix} & & & & & 1 & 1 \\ & & & & \iddots & & \\ & & 1 & 1 & & & \\ 1 & 1 & & & & & \\ 0 & 0 & & & \cdots & & 0 \\ 1 & -1 & & & & & \\ & & 1 & -1 & & & \\ & & & & \ddots & & \\ & & & & & 1 & -1 \end{bmatrix}. \tag{3}$$

B. Zero Padding and Cyclic Shifting

We have an enlarged matrix

$$\mathbf{A} = \mathbf{W}\mathbf{G}^{(0)}, \tag{4}$$

where $\mathbf{W}$ is the zero-padding and cyclically shifting matrix

$$\mathbf{W} = \begin{bmatrix} 0 & \cdots & & & \\ & & \ddots & & (N+1)/2 \\ & & & 1 & \\ 0 & & \cdots & & \\ \vdots & & & \vdots & L \quad N \\ 0 & & \cdots & & \\ 1 & & & & \\ & \ddots & & & (N-1)/2 \\ & & 1 & 0 \;\cdots & \end{bmatrix} \tag{5}$$

C. Inverse DiscreteFourier Transform

Converting $\mathbf{A}$ from the frequency domain to the time domain, we can obtain the following matrix:

$$\mathbf{P} = \mathbf{F}^{-1}\mathbf{A} = \mathbf{F}^{-1}\mathbf{W}\mathbf{G}^{(0)}, \tag{6}$$

and $\mathbf{F}$ is the DFT matrix

$$\mathbf{F} = \begin{bmatrix} 1 & 1 & 1 & \cdots & \\ 1 & e^{-j\theta} & e^{-j2\theta} & \cdots & e^{\,j\,L\,)\theta} \\ 1 & e^{-j2\theta} & e^{-j4\theta} & \cdots & e^{\,j\,L\,)\theta} \\ \vdots & \vdots & \vdots & \vdots & \vdots \\ 1 & e^{-j(L-1)\theta} & e^{-j2(L-1)\theta} & \cdots & e^{\,j\,L\quad L-1)\theta} \end{bmatrix}, \tag{7}$$

where $\theta = 2\pi / L$.

D. Jump Removing

In order to raise a pulse from a small value at the beginning point and to lower the pulse to a small value at end, the first row should be a zero vector through multiplying the jump-removing matrix $\mathbf{\Gamma}$ in the time domain [10,11] as

$$\mathbf{Q}^{+} = \mathbf{\Gamma}\mathbf{P} = \mathbf{\Gamma}\mathbf{F}^{-1}\mathbf{W}\mathbf{G}^{(0)}, \tag{8}$$

where

$$\mathbf{\Gamma} = \begin{bmatrix} 0 & 0 & & \cdots \\ -1 & 1 & & & \vdots \\ -1 & 0 & 1 & \ddots & \\ \vdots & \vdots & \ddots & \ddots & \\ -1 & 0 & \cdots & & \end{bmatrix} \tag{9}$$

The resultant jump-removed matrix $\mathbf{Q}^{+}$ becomes a matrix of size $L\times(N-1)$ as

$$\mathbf{Q}^{+}=\begin{bmatrix}\mathbf{0}\\ \mathbf{p}_2-\mathbf{p}_1\\ \vdots\\ \mathbf{p}_L-\mathbf{p}_1\end{bmatrix} \tag{10}$$

Since all the entries of the first row of this matrix **Q** are zero, the row can be discarded in order to shorten the column length. Thus, we have a $(L-1)\times(L-1)$ reduced matrix

$$\mathbf{Q}=\mathbf{W}_t\mathbf{Q}^{+}=\mathbf{\Phi}\mathbf{F}^{-1}\mathbf{W}\mathbf{G}^{(0)}=\mathbf{W}_t\mathbf{\Gamma}\mathbf{F}^{-1}\mathbf{W}\mathbf{G}^{(0)}, \tag{11}$$

where the matrix $\mathbf{W}_t$ is a $(L-1)\times(L-1)$ matrix that discards the first row as given by:

$$\mathbf{W}_t=\begin{bmatrix}0 & 1 & 0 & \cdots & \\ & & 1 & \ddots & \vdots\\ \vdots & & \ddots & \ddots & \\ 0 & & \cdots & & \end{bmatrix}. \tag{12}$$

From (11), we have

$$\mathbf{\Phi}=\mathbf{W}_t\mathbf{\Gamma}. \tag{13}$$

E. Internal Filtering Matrix

The internally filtered matrix $\mathbf{R}$ using a filtering operator $\mathbf{\Psi}$ can be represented as

$$\mathbf{R}=\mathbf{\Psi}\mathbf{Q}=\mathbf{\Psi}\mathbf{\Phi}\mathbf{F}^{-1}\mathbf{W}\mathbf{G}^{(0)}, \tag{14}$$

where $\mathbf{\Psi}$ is the $L\times(L-1)$ filtering matrix. For example, the filtering matrix with 2-tap moving average (MA) can be expressed as

$$\mathbf{\Psi}=\frac{1}{2}\begin{bmatrix}1 & & & & & \\ 1 & 1 & & & & \\ & 1 & 1 & & & \\ & & \ddots & \ddots & & \\ & & & 1 & 1 & \\ & & & & 1 & 1\\ & & & & & 1\end{bmatrix}. \tag{15}$$

The matrix $\mathbf{\Psi}$ operates in all the columns of the matrix $\mathbf{Q}$ as a filter, and it filters each column of the input matrix. Note that the length of the filtered subcarriers in the time domain should be equal or less than the IFFT size L, which means that the length of the symbol should be not increased by filtering. In an extended form, the z-transform of the MA filter with a parameter λ may be written as

$$\varsigma(z)=\frac{1}{2^{\lambda}}\left(1+z^{-1}\right)^{\lambda}. \tag{16}$$

Since the response of the subcarrier in the frequency domain is multiplied by this function, it becomes zero at both ends of the frequency band of the subcarrier.

F. Discrete Fourier Transform and Truncation

Applying DFT to each column of $\mathbf{R}$ in order to transform it from the time domain to the frequency domain, we have

$$\mathbf{B}=\mathbf{F}\mathbf{R}=\mathbf{F}\mathbf{\Psi}\mathbf{\Phi}\mathbf{F}^{-1}\mathbf{W}\mathbf{G}^{(0)}, \tag{17}$$

where **B** is a $L\times(N-1)$ matrix.

G. Downward Cyclic Shifting and Truncating

This process is cyclic shifting downwards and eliminates the rows with zero entries in order to undo zero padding and cyclic shifting by the operator **W**. Reversely cyclically shifting and truncating the matrix **B**, we have

$$\mathbf{K}=\mathbf{W}^{T}\mathbf{B}=\mathbf{W}^{T}\mathbf{F}\mathbf{\Psi}\mathbf{\Phi}\mathbf{F}^{-1}\mathbf{W}\mathbf{G}^{(0)}. \tag{18}$$

H. Nearest Orthogonal Matrix

The matrix **K** is generated through jump removing and internal filtering using $\mathbf{\Phi}$ and $\mathbf{\Psi}$ in the time domain, and $\mathbf{\Omega}$ and **S** in the frequency domain. However, even if an initial matrix $\mathbf{G}^{(0)}$ is orthogonal, the matrix **K** can be no longer guaranteed to be orthogonal. Therefore, the matrix **K** should be transformed to be orthogonal while retaining its original properties. We can obtain a filter matrix **G** which is nearest to **K** and whose columns are orthogonal to each other through the following formula [9]

$$\mathbf{G}=f(\mathbf{K})=\mathbf{K}\left(\mathbf{K}^{H}\mathbf{K}\right)^{-\frac{1}{2}}. \tag{19}$$

Since the magnitude of all the columns of the matrix **G** obtained through the function $f(\cdot)$ is 1, **G** is a special filter matrix having a constant gain in the occupied frequency band.

III. Filter Matrix with Pilot Vector

We will show how to insert a pilot vector next to the 4th column of a 9×8 jump-removed matrix below.

$$
\mathbf{U}=\begin{bmatrix}
 & & & & & & 1 & 1\\
 & & & & 1 & 1 & & \\
 & & 1 & 1 & & & & \\
1 & 1 & & & & & & \\
-2 & 0 & -2 & 0 & -2 & 0 & -2 & 0\\
1 & -1 & & & & & & \\
 & & 1 & -1 & & & & \\
 & & & & 1 & -1 & & \\
 & & & & & & 1 & -1
\end{bmatrix}. \tag{20}
$$

First, we insert an empty column vector after the 4th column of the matrix $\mathbf{U}$ and let all the remaining columns from the 5th column be one entry away from the center row as

$$
\mathbf{T}=\begin{bmatrix}
 & & & & \times & & & 1 & 1\\
 & & & & \times & 1 & 1 & \uparrow & \uparrow\\
 & & & & \times & \uparrow & \uparrow & & \\
 & & 1 & 1 & \times & & & & \\
1 & 1 & & & \times & & & & \\
-2 & 0 & -2 & 0 & \times & -2 & 0 & -2 & 0\\
1 & -1 & & & \times & & & & \\
 & & 1 & -1 & \times & & & & \\
 & & & & \times & \downarrow & \downarrow & & \\
 & & & & \times & 1 & -1 & \downarrow & \downarrow\\
 & & & & \times & & & 1 & -1
\end{bmatrix}. \tag{21}
$$

Second, we insert 1 and -1 in the fifth column so that they do not overlap with the other rows on the horizontal line, as shown in (22). The vector in the bracket of the matrix $\mathbf{T}_p$ is the pilot vector. The size of the generated matrix is thus 11×9 and as can be seen, all the columns are orthogonal to each other, so the rank becomes 9.

$$
\mathbf{T}_p=\left[\begin{array}{cccc|c|cccc}
 & & & & & & & 1 & 1\\
 & & & & & 1 & 1 & & \\
 & & & & 1 & & & & \\
 & & 1 & 1 & & & & & \\
1 & 1 & & & & & & & \\
-2 & 0 & -2 & 0 & 0 & -2 & 0 & -2 & 0\\
1 & -1 & & & & & & & \\
 & & 1 & -1 & & & & & \\
 & & & & -1 & & & & \\
 & & & & & 1 & -1 & & \\
 & & & & & & & 1 & -1
\end{array}\right]. \tag{22}
$$

IV. Frequency Responses of G-OFDM

Example 1: *G(7, 5)-OFDM*

The filter matrix used in G(7, 5) -OFDM with $\lambda = 2$ has the size of 7×5. A jump-removed matrix including a pilot vector is illustrated as

$$
\mathbf{U}_p=\left[\begin{array}{c|cccc}
 & & & 1 & 1\\
1 & & & & \\
 & 1 & 1 & & \\
0 & -2 & 0 & -2 & 0\\
 & 1 & -1 & & \\
-1 & & & & \\
 & & & 1 & -1
\end{array}\right]. \tag{23}
$$

From (19), we obtain a real filter matrix $\mathbf{G}_p^{(7\times5)}$, which is given in Table I.

TABLE I

The first column can be a pilot vector since it is not affected by other columns, and the entries $g_{2,1}$ and $g_{6,1}$ of the matrix $\mathbf{G}_p^{(7\times5)}$ can be used as the pilot symbols.

0.0000	-0.1954	0.0000	0.5116	0.7072
0.7072	0.0000	0.0000	0.0000	0.0000
0.0000	0.5117	0.7071	-0.1954	0.0000
0.0000	-0.6324	0.0000	-0.6325	0.0001
0.0000	0.5117	-0.7071	-0.1955	0.0000
-0.7070	0.0000	0.0000	0.0000	0.0000
0.0000	-0.1955	0.0000	0.5117	-0.7070

It can be seen that all entries of this matrix except the second and sixth entries of the first column are zeros, but all entries in the second and sixth rows except the first column are zeros. Since the first column is not affected by remaining columns, it can be used as the pilot vector.

Example 2: *G(73, 72)-OFDM according to the Long Term Evolution (LTE) Specifications*

Fig. 3 illustrates the frequency responses of OFDM and G-OFDM with $\lambda = 4$ according to the LTE specifications with 72 subcarriers and the frame length of $L = 128$. The magnitudes of the frequency responses of G-OFDM decrease significantly and vanish entirely at the beginning and end. This indicates that G-OFDM is less likely to have a spectral influence on neighbor channels than OFDM.

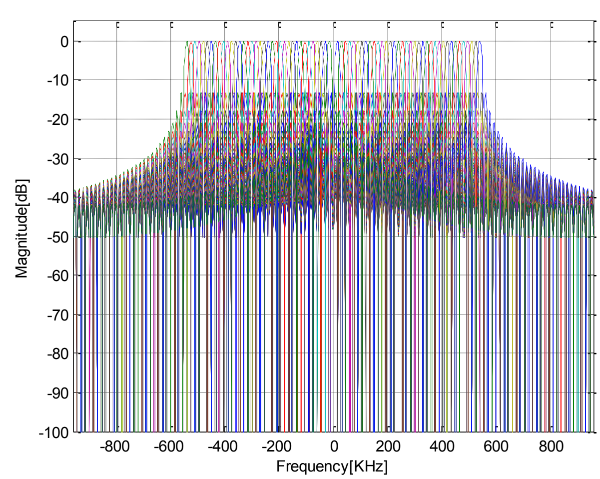

(a)

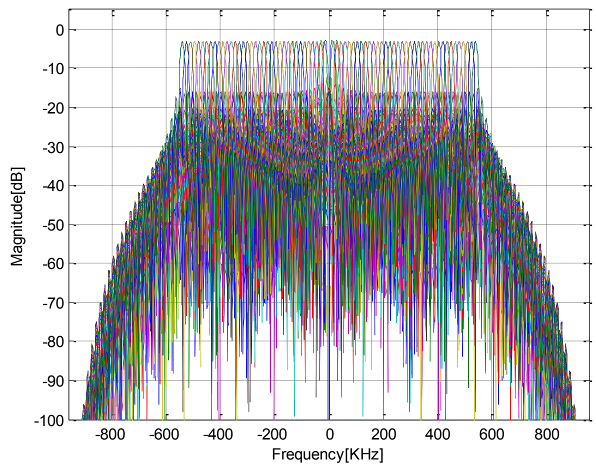

(b)

Fig. 3. Frequency response of G(73, 72)-OFDM. (a) OFDM, (b) G-OFDM

V. Crest Factor and Complementary CDF

A. Crest Factor (CF)

The signal of G-OFDM is transmitted through the IFFT after the input data symbols are band-limited through the filter matrix.

The k-th column can be represented as

$$r_k(n) = \frac{1}{L}\left[z + 2y\cos\frac{2\pi kn}{L} + 2x\sum_{l=1, l\neq k}^{(N-1)/2}\cos\frac{2\pi ln}{L}\right] \tag{24}$$

$$\text{for} \quad k = 1,2,3,\cdots \; N \quad)/2.$$

For each column of $\bar{\mathbf{\Phi}}_{\mathbf{B}}$, its IDFT can be expressed as

$$s_k(n) = \frac{j\sqrt{2}}{L}\sin\frac{2\pi kn}{L}. \tag{25}$$

The transmitted signal for G-OFDM can be represented as

$$w(n) = \sum_{k=1}^{(N-1)/2}\left[d_{2k-1}r_k(n) + d_{2k}s_k(n)\right], \tag{26}$$

where d_k is a data symbol, and $r_k(n)$ and $s_k(n)$ are real and imaginary subcarriers, respectively. We can obtain the average power

$$W(n) \equiv \sigma_d^2\left[C(n) + D(n)\right] \tag{27}$$

where $\sigma_d^2 = E\left\{\left|d_k\right|^2\right\}$ is the symbol power .

Fig. 4 shows the average power of 16 subcarriers when $N = 17$, $\sigma_d^2 = 1$ and $L = 1024$.

CF can be written as

$$C_{G-OFDM} = \left(\sum_{k=1}^{(N-1)/2}(-1)^k q_k\right)\sqrt{\frac{2}{N-1}}. \tag{28}$$

where we used that $\left|d_1\right|^2 = P_d$.

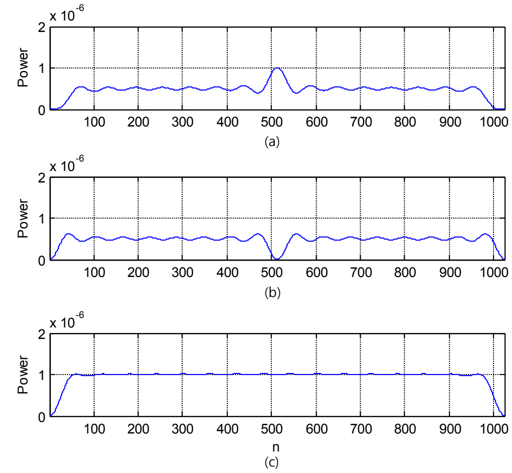

Fig.4. Signal power of G-OFDM with $\lambda = 2$. (a) Real power $C(n)$ (b) Imaginary power $D(n)$ (c) Total power $W(n)$.

The gain for CF of G-OFDM compared with OFDM becomes

$$Gain = 20\log\frac{(N-1)}{\sqrt{2}\left[\sum_{k=1}^{(N-1)/2}(-1)^k q_k\right]}. \tag{29}$$

Specifically, when $N = 4p + 1$ where p is a positive integer, the CFs of OFDM and G-OFDM become

$$C_{OFDM} = 2\sqrt{p}, \tag{30}$$

$$C_{G-OFDM} = \sqrt{2p}. \tag{31}$$

At this time, the CF gain for OFDM of G-OFDM is always as follows.

$$Gain = 20\log\frac{2\sqrt{p}}{\sqrt{2p}} = 10\log 2 \cong 3[dB].$$

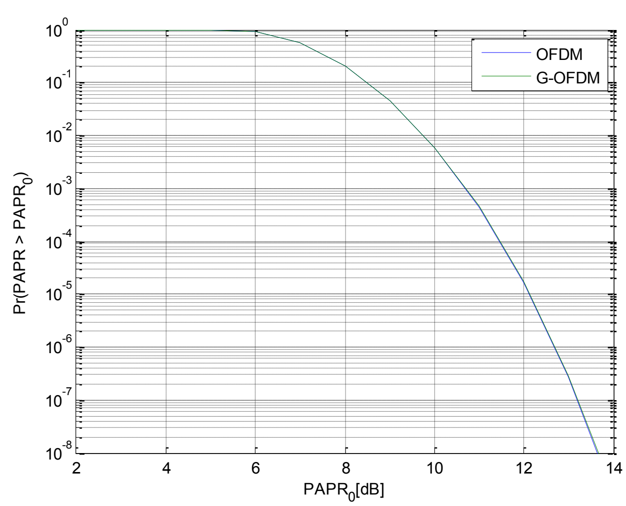

Fig. 5. CCDFs of OFDM and G-OFDM with $\lambda = 2$.

B. Complementary CDF (CCDF)

Since $w(n)$ is composed of a sum of many random signals, it can be approximated by a Gaussian distribution as

$$f\left(w(n)\right) = \exp\left(-\frac{w^2(n)}{2\sigma^2_{w(n)}}\right), \tag{32}$$

where $\sigma^2_{W(n)} = \frac{N-1}{2} E\left[w(n) w^*(n)\right]$. CCDF can be expressed as

$$P\{X > x\} = 1 - \prod_{n=1}^{L}\left(1 - \exp\left(-\frac{x^2}{2\sigma^2_{w(n)}}\right)\right). \tag{33}$$

Fig. 5 shows the CCDFs of OFDM and G-OFDM.

VI. BER Performance

The BER performance of G-OFDM with QPSK data symbols can be expressed as

$$p_b = \frac{1}{2} erfc\left(\sqrt{\frac{E_b}{N_o} \frac{tr\left(\mathbf{G}^H \mathbf{G} \mathbf{G} \mathbf{G}^H\right)}{tr\left(\mathbf{G}^H \mathbf{G}\right)}}\right), \tag{34}$$

where E_b is the energy per bit and $N_o/2$ is the noise power spectral density.

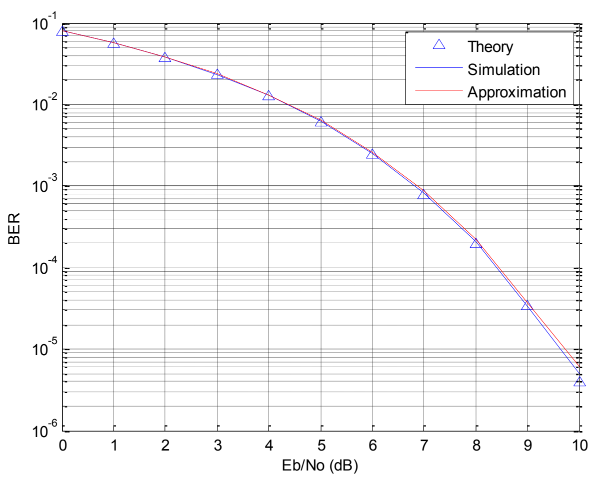

Fig. 6. BER performances of theoretical QPSK and G(73,72) -OFDM by simulation.

VII. Conclusion

We proposed a G-OFDM that could reduce the OOB leakage that was an intrinsic drawback of OFDM. G-OFDM includes filter matrices that have good spectral characteristics as well as orthogonality, which are generated through such processes as jump-removing, signal filtering, and orthogonalizing. A filter matrix consists of pilot column vectors in order to estimate multipath fading channels and remaining column vectors in order to carry data symbols. Through simulation, it was found that G-OFDM is an excellent scheme for reducing the OOB leakage effectively. Since G-OFDM filters the input symbols in the frequency domain, it is a method that can greatly reduce the amount of computation compared with any other scheme of performing convolution in the time domain. We investigated the crest factor and the complementary CDF of G-OFDM and found that the CF of G-OFDM has a gain of 3 [dB] without any PAPR reduction scheme compared with that of OFDM and the CCDF of G-OFDM has the same performance as OFDM. Through theoretical analysis and simulation, it was found that the BER performance of G-OFDM was close to the ideal BER performance, which means that the orthogonality of filter matrix does not suffer from channel noise.

The proposed scheme can be compatible with such as existing LTE or Wi-Fi systems using OFDM because it can suppress the OOB leakage without changing the length of the OFDM symbol.

References

[1] Stephen B. Weinstein, "The History of Orthogonal Frequency-Division Multiplexing," *IEEE Communications Magazine*, vol. 47, no. 11, pp. 26–35, Nov. 2009.

[2] O. Edfors, M. Sandell, J.-J. van de Beek, and S. K. Wilson, "OFDM Channel Estimation by Singular Value Decomposition," *IEEE Trans. Commun.*, vol. 46, no. 7, pp. 931-939, July 1998.

[3] Gordon L. Stüber, Steve W. Mclaughlin, Ye Li, Mary Ann Ingram, and Thomas G. Pratt, "Broadband MIMO-OFDM Wireless Communications," *Proc. IEEE*, vol. 92, no. 2, pp. 271-294, Feb. 2004.

[4] 4G Americas, "5G Spectrum recommendations," Aug. 2015.

[5] Frank Schaich, Thorsten Wild, and Yejian Chen, "Waveform Contenders for 5G - Suitability for Short Packet and Low Latency Transmissions," in *VTC Spring*, Seoul, Korea, May 2014, pp. 1-5.

[6] Frank Schaich and Thorsten Wild, "Waveform Contenders for 5G - OFDM vs. FBMC vs. UFMC," in *6th ISCCSP,* May 2014, pp. 457-460.

[7] Myungsup Kim and Do Young Kwak, "Generalized OFDM for 5th Generation Mobile Communication." Accepted paper, *VTC2017-Spring*, 2017.

[8] Nicola Michailow, Maximilian Matthé, Ivan Simões Gaspar, Ainoa Navarro Caldevilla, Luciano Leonel Mendes, Andreas Festag, and Gerhard Fettweis, "Generalized Frequency Division Multiplexing for 5th Generation Cellular Networks," *IEEE Trans. Commun.*, vol. 62, no. 9, pp. 3045-3059, Sep. 2014.

[9] Nicholas J. Higham, "Computing the Polar Decomposition - With Applications*," *SIAM J. SCI. STAT. COMPUT*. vol. 7, no. 4, Oct. 1986

[10] Myungsup Kim and Do Young Kwak, " A Pilot Included Column Mean Vanishing Matrix," *Journal of Mathematics Research*, Vol. 9, No. 2, pp. 128 – 133, April 2017.

[11] Myungsup Kim and Do Young Kwak, "Column Mean Vanishing Matrices," *International Journal of Pure and Applied Mathematics*, Vol. 114, No. 3, pp. 457 – 471, May 2017.